Laser Phys. Lett. **00** (2015) 000000 (6pp) UNCORRECTED PROOF

80 GHz waveform generated by the optical Fourier synthesis of four spectral sidebands

Julien Fatome, Kamal Hammani, Bertrand Kibler and Christophe Finot

Laboratoire Interdisciplinaire Carnot de Bourgogne, UMR 6303 CNRS-Université de Bourgogne Franche-Comté, 9 Avenue Alain Savary, BP 47870, 21078 Dijon Cedex, France

E-mail: christophe.finot@u-bourgogne.fr

Received 17 September 2015, revised 6 November 2015
Accepted for publication 6 November 2015
Published

Abstract

Using the linear phase shaping of a simple four-line optical frequency comb, we experimentally demonstrate the generation of various optical waveforms such as parabolic, triangular or flat-top pulse trains at a repetition rate of 80 GHz. The initial 80 GHz comb is obtained through the nonlinear spectral broadening of a 40 GHz carrier-suppressed sinusoidal beating in a highly nonlinear fiber. Proof-of-principle experiments are reported for two distinct configurations of the waveform generated: continuous trains and bunches of shaped pulses.

Keywords: optical pulse shaping, nonlinear fiber optics, waveform generation

AQ1 (Some figures may appear in colour only in the online journal)

1. Introduction

Versatile and easy-to-implement ways of generating arbitrary optical waveforms at high repetition rates are of considerable interest for applications in optical communications, all-optical signal processing, instrumentation systems and microwave signal manipulation [1, 2]. Although shaping sinusoidal, Gaussian or hyperbolic secant intensity profiles is commonly achieved by means of modulators or mode-locked lasers, other pulse profiles such as parabolic, triangular or flat-top shapes remain challenging to synthesize. In this context, several strategies have already been explored. First, linear pulse shaping is a common method of carving an initial ultrashort pulse train into the desired shape. In this case, the transfer function is given in the spectral domain by the ratio between the target field and the initial optical field. The linear shaping of picosecond pulses has been demonstrated by means of numerous components, including spatial light modulators [3, 4], superstructured-fiber Bragg gratings [5], acousto-optic devices [6] and arrayed waveguide gratings [7]. Furthermore, the line-by-line shaping of a coherent frequency comb made of tens of spectral components has also been investigated for generating more complex structures [8], whereas the Fourier synthesis of a few discrete frequency spectra has been exploited to generate high-fidelity ultrafast periodic intensity profiles efficiently [9–11].

Besides linear shaping techniques, several nonlinear methods have been implemented in order to benefit from the adiabatic evolution of the intensity pulse profile upon propagation in optical fibers. For instance, high-quality parabolic intensity profiles [12] or triangular shapes [13, 14] have been generated thanks to the combined effects of Kerr nonlinearity and normal dispersion. Other examples of efficient methods are based on photonic generation involving specific Mach–Zehnder modulators [15, 16] and microwave photonic filters [17] as well as frequency-to-time conversion [18, 19].

Recently, we theoretically and experimentally demonstrated a new linear approach enabling the synthesis of periodic high-repetition-rate pulses with various intensity profiles ranging from parabola to triangular and flat-top [20]. By using only four comb lines resulting from a phase-modulated continuous wave, we successfully demonstrated the generation of high-fidelity ultrafast periodic waveforms at 40 GHz. In the present work, after recalling the operational principle of this approach, we describe a new scenario for obtaining the required initial spectrum by taking advantage of the four-wave mixing process occurring in a highly nonlinear fiber (HNLF). This concept is experimentally validated at a repetition rate of 80 GHz, and the generation of a bunch of shaped pulses is then investigated.

 © 2015 Astro Ltd Printed in the UK

JNL:LPL PIPS: AA096E TYPE: LET TS: NEWGEN DATE:20/11/15 EDITOR: IOP SPELLING: US

2. Principle of operation

2.1. Waveform synthesis based on four spectral lines

When considering a temporal train of symmetric pulses, the corresponding four-band optical spectrum is also expected to be symmetric and only two parameters are therefore required to mathematically describe such a spectrum. As illustrated in figure 1, the first parameter is the ratio A between the amplitude of the central components and the amplitude of the lateral sidebands. The second parameter consists of the spectral phase φ of the lateral sidebands relative to the central components.

From this particular spectrum, it is easy to retrieve the analytical expression of the temporal intensity profile [20] given by:

$$I(t) = 2[1 + A^2 + (1 + 2A\cos(\varphi))\cos(\omega_0 t) + 2A\cos(\varphi)\cos(2\omega_0 t) + A^2\cos(3\omega_0 t)] \quad (1)$$

with $\omega_0 = 2\pi R$, R being the repetition rate of the pulse train. By exploring the bi-dimensional space (A^2, φ) (figure 2(a)), we notice that the degree of kurtosis excess [21] calculated over one period of the generated pulse train varies significantly. It may reach positive or negative values. This implies that very different levels of peaked-ness can be reached, allowing for the synthesis of numerous temporal intensity shape profiles. Indeed, we previously demonstrated that operating at a value A^2 of -12 dB is particularly appealing as it enables us to switch directly between parabola, rectangular, flat-top or even dark parabola temporal intensity profiles by simply varying the spectral phase parameter φ [20].

In order to complement the kurtosis excess at $A^2 = -12$ dB (see figure 2(b)) and to characterize more accurately the generated pulse shape, we also evaluated the misfit factor M between the synthesized pulse shape $I(t)$ and a fit by the targeted intensity profile I_{fit} where I_{fit} can be a parabolic or triangular waveform:

$$M^2 = \int (I - I_{\text{fit}})^2 \mathrm{d}t \,/\, \int I^2 \mathrm{d}t \quad (2)$$

Numerical results are depicted in figure 2, panel (c). Misfit factors below 0.03 are reached for $\varphi = 1.52$ rad and $\varphi = 1.92$ rad (triangular and parabolic waveforms respectively, points B and A of figure 2) indicate that high-quality pulse profiles can be synthesized. Details of the resulting intensity profiles are reported in figures 3(a) and (b) for a repetition rate R of 80 GHz and confirm the very good agreement between the generated profiles and the desired shapes (the fits are plotted with filled grey circles). Nevertheless, the temporal chirp profile, also plotted in figure 3, reveals that the generated pulses are far from being Fourier transform-limited or even linearly chirped. Actually, in contrast with conventional schemes that aim to carve both temporal and phase profiles in the spectral domain, in our bi-dimensional analysis we do not take into account any constraint on the temporal phase profile for the generated pulses. For other operating points C, D and E (corresponding to $\varphi = 2.21$, 0.7, and 3.1 rad respectively), dark parabolic, flat-top and double-peaked waveforms are respectively generated as illustrated in panels (c) and (e) of figure 3.

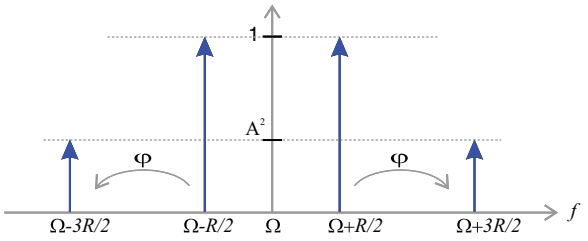

Figure 1. Optical spectrum of a four-band model. Ω is the carrier frequency and R is the repetition rate.

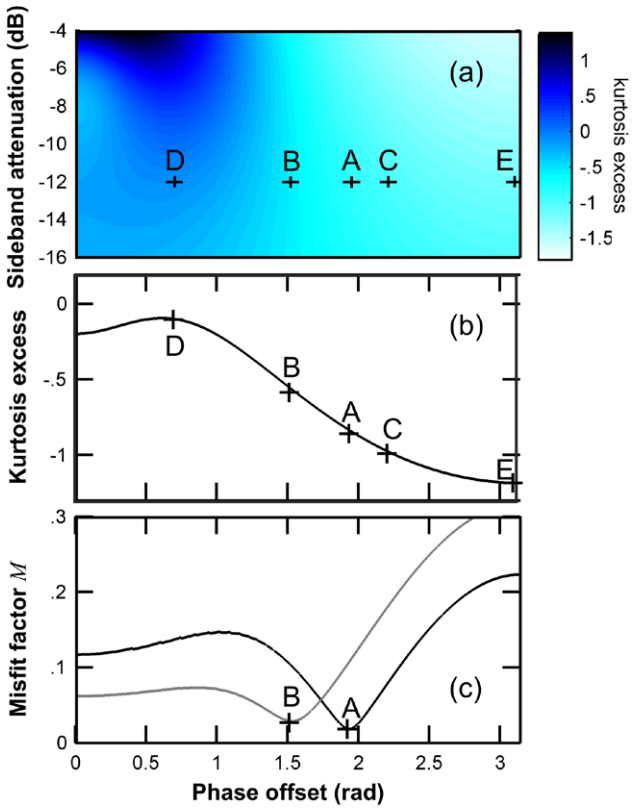

Figure 2. (a) Evolution of the kurtosis excess according to the phase difference φ and attenuation A^2 of the outer sidebands with respect to the inner sidebands. (b) Details of the evolution of the kurtosis excess according to φ for a fixed sideband ratio A^2 of -12 dB. (c) Evolution of misfit factor M according to φ for a fixed sideband ratio A^2 of -12 dB and for a parabolic and triangular target (black and grey lines respectively). Points A, B, C, D and E are the parameters used in the sub-plots (a)–(e) of figure 3, respectively.

2.2. Generation of the initial four spectral sidebands

Our approach relies on the phase shaping of a symmetric spectrum made of four spectral lines having a ratio A^2 of -12 dB. In a previous proof-of-principle experiment [20], such a spectrum was obtained through the phase modulation of a continuous wave at 20 GHz. The approach was not really power efficient as half of the spectral components had to be removed. Moreover, the scaling of this technique to repetition rates of higher than 40 GHz becomes technically challenging due to the bandwidth limitation of current optoelectronic devices. To overcome this issue, we propose here an alternative solution

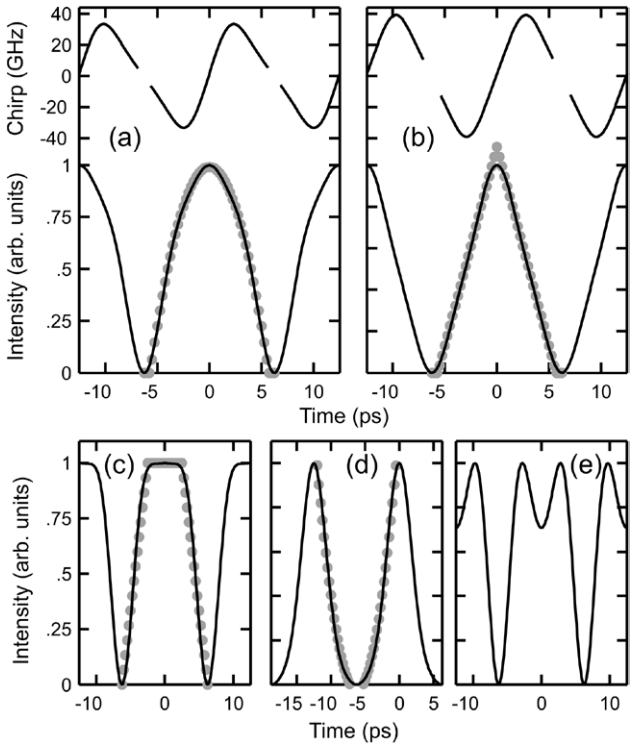

Figure 3. Various pulse shapes of the 80 GHz repetition rate pulse train obtained numerically for a sideband ratio A^2 of -12 dB. (a) and (b) Temporal intensity and phase profiles obtained for points A and B of figure 2 leading to the generation of parabolic and triangular pulse trains respectively. (c)–(e) Other temporal intensity profiles generated for a phase difference φ of 2.24, 0.70 and 3.1 rad (points C, D and E): flat-top pulse, dark parabolic profile, double-peaked structure. The intensity profile is compared with a fit by the target waveform (solid grey circles).

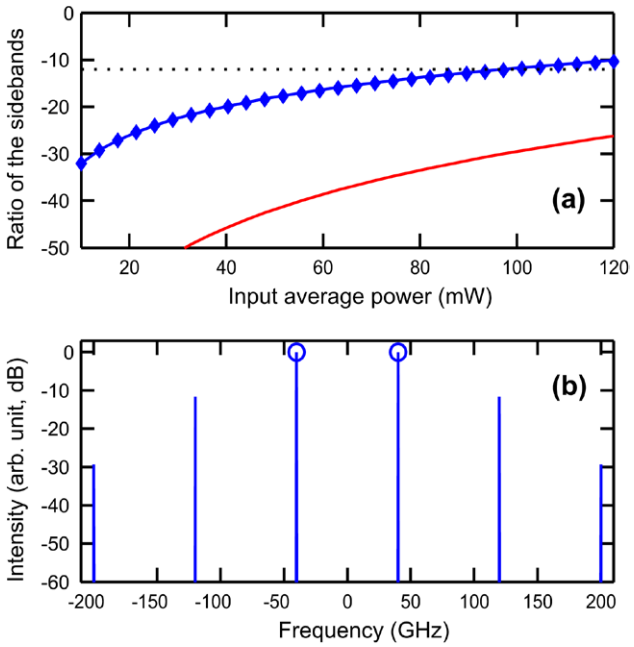

Figure 4. (a) Evolution of the ratio between the intensity of the central and first as well as the second lateral sidebands of the output spectrum according to the input average power (blue and red lines respectively). The dotted line represents the target of -12 dB. The diamonds represent the analytical predictions [22]. (b) The optical spectrum before and after propagation in a 1 km long HNLF (circle and solid line respectively) for an input average power leading to a -12 dB ratio between the central and first lateral sidebands.

that takes advantage of the nonlinear propagation of a sinusoidal beating in an optical fiber.

In order to illustrate such an approach, we first numerically consider the evolution of a carrier-suppressed 80 GHz sinusoidal beat-signal in a highly nonlinear fiber having a second order dispersion coefficient of 0.5 ps km^{-1} nm^{-1} and a nonlinear coefficient γ of 10 W km^{-1}. We performed numerical simulations of the propagation along the distance $L = 1$ km based on the standard nonlinear Schrödinger equation. The four-wave mixing process between the two initial spectral components creates new symmetric and regularly spaced sidebands. Figure 4(a) summarizes the evolution of the ratio A^2 (solid blue line) according to the initial average power P_0. The targeted ratio of -12 dB can be reached for an input power of 100 mW. The results of the numerical simulations are in full agreement with the theoretical prediction of Boskovic *et al* [22] assuming a pure self-phase modulation effect (blue diamonds) where the ratio A^2 is predicted by:

$$A^2 = \frac{J_0(\phi/2)^2 + J_1(\phi/2)^2}{J_1(\phi/2)^2 + J_2(\phi/2)^2} \tag{3}$$

where ϕ is the nonlinear phase given by $\phi = \gamma P_0 L$. This is consistent with the fact that for this range of parameters, the regime of propagation is mainly driven by Kerr nonlinearity, and contrary to [8, 12, 23, 24] the temporal intensity profile is not modified upon propagation here.

Details of the spectrum generated with 100 mW pump power are given in figure 4(b) and reveal that due to the multiple four-wave mixing process, additional lateral spectral components are generated at 200 GHz. However, their level remains below -30 dB compared to the level of the inner sidebands and we checked that their presence did not impair the expected reshaping. For this range of parameters, there is no signature of modulation instability that could degrade the coherence of the signal [25]. Another noticeable point is that the spectral components are not in phase in contrast with the spectrum resulting from a pure sinusoidal phase modulation of a continuous wave [26].

3. Generation of a continuous train of shaped pulses

We first investigate the generation of a continuous train of shaped pulses at a repetition rate R of 80 GHz.

3.1. Experimental setup

In order to experimentally validate the feasibility of our approach, we implemented a setup based exclusively on commercially available components operating at telecommunication wavelengths as depicted in figure 5. A continuous-wave laser (an external-cavity laser diode) is first intensity-modulated using a lithium-niobate intensity modulator electrically driven

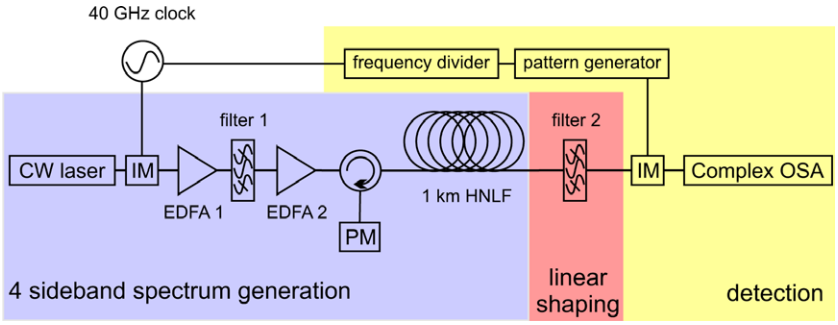

Figure 5. Experimental setup: CW—continuous wave, IM—intensity modulator, EDFA—erbium-doped fiber amplifier, PM—power meter, HNLF—highly nonlinear fiber, OSA—optical spectrum analyser.

by a 40 GHz sinusoidal clock and operating at the point of null-transmission. The modulated signal is then amplified by means of a low noise erbium-doped fiber amplifier (EDFA), followed by a programmable optical bandpass filter that partly removes the amplified spontaneous noise emission and limits the energy contained in the central carrier component.

A second EDFA is then used to reach the power level required for the generation of the additional pair of lateral sidebands through the self-phase modulation effect occurring in the highly nonlinear fiber whose physical parameters correspond to the one involved in the numerical results described in the above numerical analysis. In order to prevent the deleterious effects of Brillouin backscattering, an optical circulator is inserted at the fiber input while a power-meter monitors the reflected power. The Brillouin threshold has thereby been experimentally evaluated around 60 mW.

After this stage of nonlinear propagation, a second programmable optical filter based on liquid crystal on silicon (LCOS) technology (Finisar waveshaper device) [4] is then implemented so as to imprint the targeted shaping on the four-line comb spectrum. Intensity and chirp characterization are achieved using a complex optical spectrum analyzer (APEX technologies, AP2441) that requires the signal to be periodically modulated at a repetition rate of 2.5 GHz or 625 MHz. In order to fulfill this technological requirement, we frequency-divided the initial 40 GHz clock to obtain a 10 GHz clock that then drives a pattern generator delivering a 1011 pattern at 10 GHz.

3.2. Experimental results

The spectrum recorded at the input of the HNLF with the high-resolution optical spectrum analyzer is plotted in figure 6(a). As expected from an intensity modulator operating at its null transmission point, the spectrum of the resulting carrier-suppressed signal clearly exhibits two components that are separated by twice the initial clock frequency and that are symmetrically located with respect to the residual central spectral line (the extinction ratio of this unwanted component is higher than 30 dB).

The expanded spectrum that is obtained after propagation in the HNLF for an input power of 60 mW (17.8 dBm) is plotted in figure 6(b). The expected new lateral sidebands are clearly visible. Given the power limitation associated with Brillouin scattering, the ratio between the main inner and

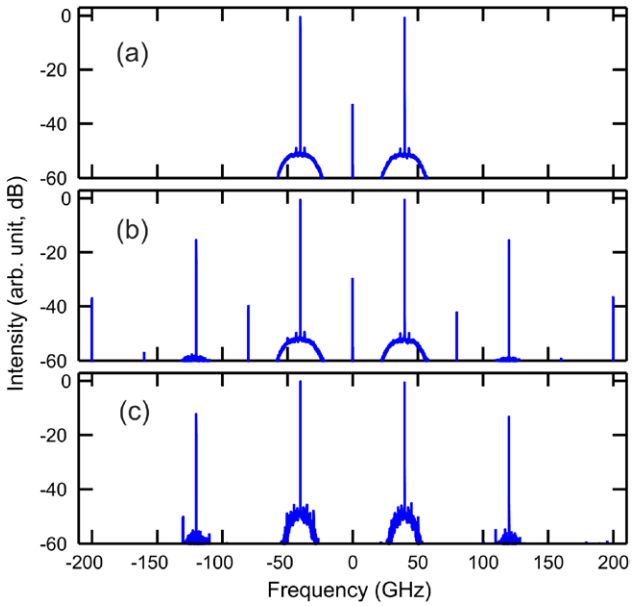

Figure 6. Optical spectrum recorded (a) before the HNLF, (b) after the HNLF and (c) after filter two. Frequencies of the optical spectra are relative to the carrier frequency (193.4 THz).

outer sidebands is limited to −15.6 dB, which is fully consistent with the numerical simulations discussed in section 2. Note that several approaches, such as the phase modulation of the input pump [27], longitudinal strain or temperature distribution [28–30], as well as aluminum-doped HNLF [31] may be implemented to overcome Brillouin limitation. We also tested other highly nonlinear fibers with the same length and nonlinearity but distinct normal and anomalous dispersion values. Similar results were obtained, thus confirming that self-phase modulation is the main process driving spectral expansion here.

The spectrum obtained after linear spectral shaping is displayed in figure 6(c). By selectively adding a 3.6 dB attenuation to the inner sidebands, we achieved the targeted 12 dB ratio. We also removed the residual central line as well as the other spurious sidebands in order to keep only the four significant spectral components we needed and to limit pulse-to-pulse fluctuations. An optical signal-to-noise ratio better than 47 dB was then achieved. Note that at this stage of linear shaping, the programmable optical filter also imprints the phase difference between the various spectral components.

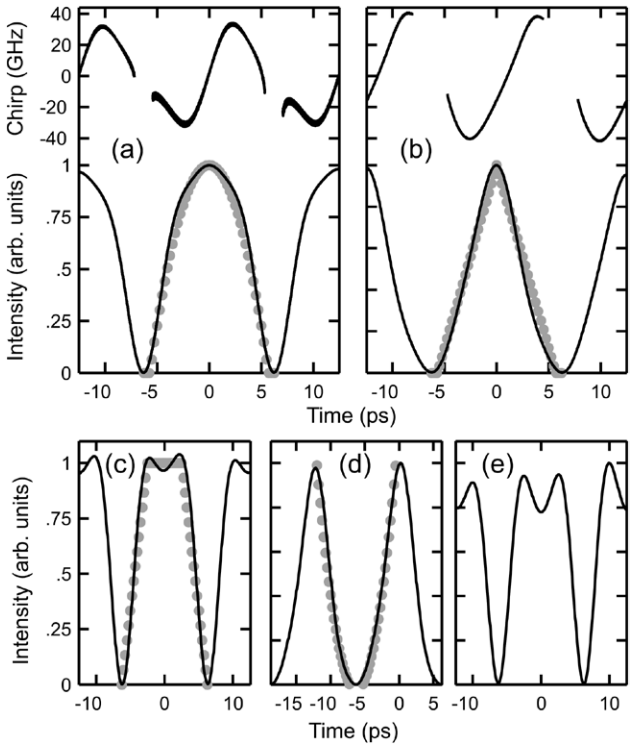

Figure 7. Various pulse shapes obtained experimentally for a spectral ratio A^2 of −12 dB and plotted over two periods. (a) and (b) The temporal intensity and phase profiles corresponding to the parabolic and triangular pulse trains respectively. (c)–(e) Other temporal intensity profiles obtained experimentally: flat-top pulse, dark parabolic profile, double-peaked structure. The intensity profile is compared with the same fit as the one used in figure 3 (solid grey circles). The small pulse-to-pulse fluctuations that are observed may be partly attributed to the detection setup that requires the use of a second intensity modulator.

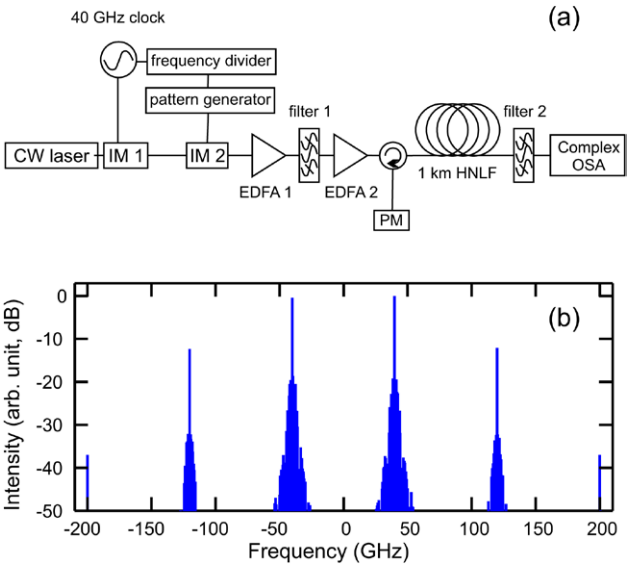

Figure 8. (a) Experimental setup (same acronyms as in figure 5). (b) Experimental spectrum obtained after filter two and recorded on a high-resolution spectrum.

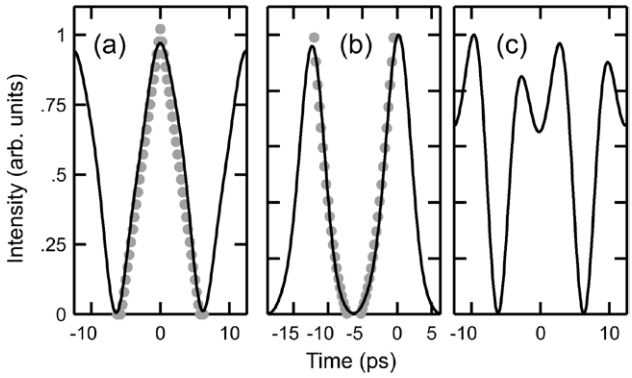

Figure 9. Various pulse shapes obtained experimentally in the case of a bunch of eight temporal periods: (a) triangular pulse, (b) dark parabolic profile and (c) double-peaked structure. The intensity profile is compared with the same fit as the one used in figure 3 and figure 7 (solid grey circles). The small pulse-to-pulse fluctuations that are observed may be partly attributed to the use of two cascaded intensity modulators.

The results of the temporal characterization obtained for various phase detunings φ are presented in figure 7 and demonstrate the generation of the expected pulse shapes at a repetition rate of 80 GHz. For illustration, high-quality parabolic profiles are successfully achieved (figure 7(a)), as well as triangular pulses (figure 7(b)). The intensity profiles are in close agreement with the same parabolic or triangular fits as the one used in figure 3).The chirp profiles can also be compared with the ones predicted by numerical simulations and exhibit the same trends. It is noteworthy that simply changing φ here is sufficient to switch from one pulse shape to another, making the present method easily reconfigurable and of high practical interest. The generation of trains of pulses with a high level of flatness can also be observed in figure 7(c), as well as a train of dark parabola (figure 7(d)) or double-peaked structures (figure 7(e)).

4. Generation of a bunch of shaped pulses

After the demonstration of a continuous train of shaped pulses at 80 GHz, we now investigate the generation of a train of shaped pulses with a temporal finite extension. For this purpose, we modified the experimental setup of figure 5 to the setup sketched in figure 8(a). More precisely, after the generation of the initial sinusoidal beating, the second optical intensity modulator selects a sequence of eight oscillations. This bunch of pulses is repeated at a rate of 625 MHz, leading to a 12 dB reduction in terms of average power at the input of the HNLF. With such a power reduction, it was possible to reach a ratio of −12 dB between the main inner and outer sideband without suffering from any Brillouin backscattering. Consequently, the spectral intensity reshaping by the second programmable filter is then no longer required. Only the phase shaping of the four-line comb spectrum was exploited here. Note that further optimization of the setup should also enable us to get rid of the second amplifier stage. AQ2

In this configuration, as shown in figure 8(b), and contrary to the results obtained in the case of a continuous pulse train, the sidebands are no longer composed of a single spectral line. Indeed, the repetition rate of the bunch leads to a comb structure of each sideband with a spectral spacing of 625 MHz.

The spectral extension of the sidebands is directly linked to the duration of the bunch of pulses. Note that with eight pulses included within a bunch, the spectral width of each sideband is much lower than the repetition rate of the pulse source (80 GHz), leading to well-separated sidebands. Since the main four sidebands do not overlap, imprinting a clear phase difference between the inner and outer ones can still be experimentally achieved. A set of various temporal intensity profiles that were experimentally synthesized is presented in figure 9 and does not show any degradation compared to the previous case of the shaping of a continuous train.

5. Conclusion

In conclusion, we have demonstrated the generation of 80 GHz high-repetition-rate pulse trains based on the linear phase shaping of a single four-sideband spectrum. The efficiency as well as the reconfigurable property of this photonic waveform generator was experimentally validated by various high-quality intensity profiles recorded at 80 GHz. In particular, parabolic, triangular or flattened waveform intensity shapes as well as their associated chirp profiles were successfully reported and compared with the theoretical predictions. Compared to our previous results reported in [20], the present work represents a two-fold improvement in the repetition rate that can be achieved by means of this technique. This progress has been made possible by taking advantage of the four-wave mixing process occurring during the propagation of a 40 GHz beat-signal in a highly nonlinear fiber. More precisely, the self-phase modulation induced by this carrier-suppressed sinusoidal signal generates the outer spectral components with an adequate amplitude ratio with respect to the inner spectral components. We also checked that our method was not only restricted to continuous wave trains and that bunches of shaped pulses could also be synthesized.

In order to provide this first proof-of-principle demonstration, we focused our work on periodic bunches–but it is worth mentioning that periodicity is not required, especially for data-packet applications. Moreover, to obtain the initial bi-chromatic pump, we exploited an intensity modulator operating at its null transmission point. However, to reach higher repetition rates and to relax the optoelectronic bandwidth limitation, the coherent combination of two continuous signals generated from different lasers [10, 11], bi-chromatic lasers [32], multi-frequency Brillouin oscillators [33] or the micro-resonator-based generation of stable coherent combs with frequency spacing above 100 GHz [34] appear to be various promising solutions.

Acknowledgments

We acknowledge the financial support of the Conseil Regional de Bourgogne (Pari Photcom) and the funding of the Labex ACTION program (ANR-11-LABX-0001-01) and the European Regional Development Fund. The experimental work benefited from the PICASSO Platform of the University of Burgundy.

References

AQ3

[1] Boscolo S and Finot C 2012 *Int. J. Opt.* 159057 AQ4
[2] Yao J P 2011 *Opt. Commun.* **284** 3723–36
[3] Cundiff S T and Weiner A M 2010 *Nat. Photonics* **4** 760–6
[4] Clarke A M, Williams D G, Roelens M A F and Eggleton B J 2010 *J. Lightwave Technol.* **28** 97–103
[5] Parmigiani F, Petropoulos P, Ibsen M and Richardson D J 2006 *IEEE Photonics Technol. Lett.* **18** 829–31
[6] Andresen E R, Dudley J M, Finot C, Oron D and Rigneault H 2011 *Opt. Lett.* **36** 707–9
[7] Hirooka T, Nakazawa M and Okamoto K 2008 *Opt. Lett.* **33** 1102–4
[8] Frisquet B, Chabchoub A, Fatome J, Finot C, Kibler B and Millot G 2014 *Phys. Rev.* A **89** 023821
[9] Chan H S, Hsieh Z M, Liang W H, Kung A, Lee C K, Lai C J, Pan R P and Peng L H 2011 *Science* **331** 1165–8
[10] Wu D S, Richardson D J and Slavik R 2015 *Optica* **2** 18–26
[11] Hyodo M, Abedin K and Onodera N 2000 *Electron. Lett.* **36** 224–5
[12] Finot C, Fatome J, Pitois S and Millot G 2007 *IEEE Photonics Technol. Lett.* **19** 1711–3
[13] Boscolo S, Latkin A I and Turitsyn S K 2008 *IEEE J. Quantum Electron.* **44** 1196–203
[14] Bale B G, Boscolo S, Hammani K and Finot C 2011 *J. Opt. Soc. Am.* B **28** 2059–65
[15] Jing L, Tigang N, Li P, Wei J, Haidong Y, Hongyao C and Chan Z 2013 *IEEE Photonics Technol. Lett.* **25** 952–4
[16] Zhang F, Ge X and Pan S 2013 *Opt. Lett.* **38** 4491–3
[17] Li W, Wang W T, Sun W H, Wang W Y and Zhu N H 2014 *Opt. Express* **22** 14993–5001
[18] Ye J, Yan L, Pan W, Luo B, Zou X, Yi A and Yao S 2011 *Opt. Lett.* **36** 1458–60
[19] Jiang Y, Ma C, Bai G, Qi X, Tang Y, Jia Z, Zi Y, Huang F and Wu T 2015 *Opt. Express* **23** 19442–52
[20] Finot C 2015 *Opt. Lett.* **40** 1422–5
[21] Kenney F and Keeping E 1951 *Mathematics of statistics: Part 2* (Princeton, NJ: D. Van Nostrand)
[22] Boskovic A, Chernikov S V, Taylor J R, Gruner-Nielsen L and Levring O A 1996 *Opt. Lett.* **21** 1966–8
[23] Fatome J, Finot C, Millot G, Armaroli A and Trillo S 2014 *Phys. Rev. X* **4** 021022
[24] Fortier C, Kibler B, Fatome J, Finot C, Pitois S and Millot G 2008 *Laser Phys. Lett.* **5** 817–20
[25] Fatome J, Finot C, Armaroli A and Trillo S 2013 *Opt. Lett.* **38** 181–3
[26] Trillo S, Wabnitz S and Kennedy T 1994 *Phys. Rev.* A **50** 1732–47
[27] Lichtman E, Waarts R G and Friesem A A 1989 *IEEE J. Lightwave Technol.* **7** 171–4
[28] Yoshizawa N and Imai T 1993 *IEEE J. Lightwave Technol.* **11** 1518–22
[29] Chavez Boggio J M, Marconi J D and Fragnito H L *IEEE J. Lightwave Technol.* **23** 3808–14
[30] Imai Y and Shimada N 1993 *IEEE Photonics Technol. Lett.* **5** 1335–7
[31] Gruner-Nielsen L, Jakobsen D, Herstrom S, Palsdottir B, Dasgupta S, Richardson D J, Lundstrom C, Olsson S and Andrekson P 2012 *38th European Conf. and Exhibition on Optical Communications*
[32] Yu L, Zhou D and Zhao L 2014 *Laser Phys. Lett.* **11** 095404
[33] Buttner T F, Kabakova I V, Hudson D D, Pant R, Poulton C G, Judge A C and Eggleton B J 2014 *Sci. Rep.* **4** 5032
[34] Ferdous F, Miao H, Leaird D E, Srinivasan K, Wang J, Chen L, Varghese L T and Weiner A M 2011 *Nat. Photonics* **5** 770–6

QUERIES

Page 1
AQ1
Please be aware that the colour figures in this article will only appear in colour in the online version. If you require colour in the printed journal and have not previously arranged it, please contact the Production Editor now.
Page 5
AQ2
Please check the edits made to the sentence "After the demonstration of a continuous train..."
Page 6
AQ3
Please check the details for any journal references that do not have a link as they may contain some incorrect information.
AQ4
Please provide the volume for reference [1].